CHINA SPALLATION NEUTRON SOURCE DESIGN*

J. Wei†[3,1], S.-X. Fang[1], J. Feng[2], S.-N. Fu[1], H.-F. Ouyang[1], Q. Qin[1], H.-M. Qu[1], J.-Y. Tang[1], F.-W. Wang[2], S. Wang[1], Z.-X. Xu[1], Q.-W. Yan[2], J. Zhang[2], Z. Zhang[2]
for the China Spallation Neutron Source (CSNS) teams
Institute of High Energy Physics, China[1]; Institute of Physics, China[2];
Brookhaven National Laboratory, USA[3]

Abstract

The China Spallation Neutron Source (CSNS) is an accelerator-based high-power project currently in preparation under the direction of the Chinese Academy of Sciences (CAS). The complex is based on an H^- linear accelerator, a rapid cycling proton synchrotron accelerating the beam to 1.6 GeV, a solid tungsten target station, and five initial instruments for spallation neutron applications. The facility will operate at 25 Hz repetition rate with a phase-I beam power of about 120 kW. The major challenge is to build a robust and reliable user's facility with upgrade potential at a fractional of "world standard" cost.

INTRODUCTION

There exist three classes of high-power spallation neutron facilities[1, 2]: continuous-wave (CW) facilities driven by high energy, high intensity cyclotrons or linacs (e.g. the operating SINQ isochronous-cyclotron at PSI with a beam power of 1.2 MW at 590 MeV [3]); long-pulse (ms) facilities driven by high energy, high intensity linacs (e.g. the operated LAMPF proton linac with a beam power of 1 MW at 800 MeV [4] and the PEFP under construction in Korea with a high-duty 100 MeV linac [5]); and short (μs) pulse facilities driven by a combination of high intensity linacs and rings, as shown in Fig. 1 [4, 6, 7, 2]. Among the short-pulse facilities are two types of accelerator layout: a full-energy linac followed by an accumulator (e.g. the operating LANSCE linac and PSR with a beam power of 80 kW at 800 MeV [4] and the SNS project just commissioned at ORNL with a 1 GeV superconducting (SC) RF linac and an accumulator [8]) and a partial-energy linac followed by a rapid cycling synchrotron (RCS) (e.g. the operating ISIS facility at RAL with a beam power of 160 kW from a 70 MeV linac and a 800 MeV synchrotron [9] and the J-PARC under construction in Japan with a 400 MeV linac and 3 GeV and 50 GeV synchrotrons [10]).

CSNS is an accelerator-based short-pulse facility with a partial-energy linac followed by a RCS. CSNS provides a multidisciplinary platform for scientific research and applications by national institutions, universities, and industries [12, 13, 14]. The high-flux pulsed neutrons from CSNS will compliment cw neutrons from nuclear reactors and synchrotron lights from synchrotron radiation facilities. Strongly advocated by the users groups, the CSNS project was approved by the Chinese central government in 2005.

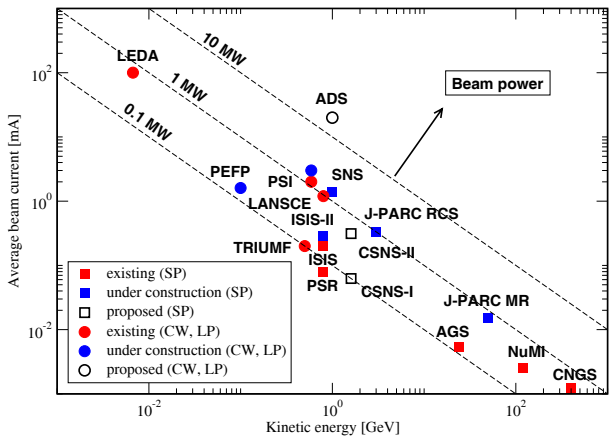

Figure 1: Accelerators at the power frontier (short pulse SP, long pulse LP, continuous wave CW).

As shown in Fig. 1 and Table 1, the CSNS accelerator is designed to deliver a beam power of 120 kW with the upgrade capability of up to 500 kW by raising the linac output energy and increasing the beam intensity.

Table 1: CSNS accelerator primary parameters.

Project Phase	**I**	**II**	**II'**
Beam power on target [kW]	120	240	500
Proton energy on target [GeV]	1.6	1.6	1.6
Average beam current [μA]	76	151	315
Pulse repetition rate [Hz]	25	25	25
Proton per pulse on target [10^{13}]	1.9	3.8	7.8
Pulse length on target [ns]	<400	<400	<400
Linac output energy [MeV]	81	134	230
Ion source/linac length [m]	50	76	86
Linac RF frequency [MHz]	324	324	324
Macropulse ave. current [mA]	15	30	40
Macropulse duty factor [%]	1.1	1.1	1.7
LRBT length [m]	142	116	106
Synchrotron circumference [m]	230.8	230.8	230.8
Ring filling time [ms]	0.42	0.42	0.68
Ring RF frequency [MHz]	1.0-2.4	1.3-2.4	1.6-2.4
Max. uncontr. beam loss [W/m]	1	1	1
Target material	tungsten		
Moderators	H_2O, CH_4, H_2		
Number of spectrometers	5	18	>18

* Work performed under the auspices of the Chinese Academy of Sciences (CAS) and the U.S. Department of Energy.

† weijie@ihep.ac.cn and jwei@bnl.gov

Figure 2: Artist's layout of the CSNS complex.

The CSNS complex operates at a repetition rate of 25 Hz producing spallation neutrons by striking the metal target with proton beams. Initially, the H^- beam is produced from the ion source, and then pre-chopped and transported through the LEBT. The beam is then bunched and accelerated through the RFQ at a RF frequency of 324 MHz. The MEBT accepts the 3 MeV beam from the RFQ, further chops the beam to the ring RF period, and matches the beam to the DTL. At phase I of the project, the DTL accelerates the beam to 81 MeV. The LRBT transport contains empty drift spaces for future addition of linac modules (DTL or superconducting RF) for the linac energy and beam power upgrade. Upon collimation in both the transverse and longitudinal directions in the LRBT, the H^- beam is stripped of the electrons and injected by phase-space painting into the RCS ring. The ring accumulates and then accelerates the proton beam to 1.6 GeV. The beam is extracted in a single turn and delivered to the target through the RTBT transport (Fig. 2, [12]). Upon striking the solid tungsten target, each proton produces 20 to 30 neutrons through spallation process. These neutrons are slowed down to the desired energies through three types of moderators (H_2O, liquid CH_4, and liquid H_2) for neutron scattering experiments.

Financially, the project must fit in China's present economical condition with a cost of about 1.5 billion Chinese Yuan (CNY) (about US$0.2 B). This limits the initial beam power to about 120 kW. On the other hand, we strive to reserve the upgrade potential up to 500 kW so that the facility is competitive in future. Since this is the first high-intensity proton machine in China, we intend to adopt mature technology as much as possible.

The CSNS complex is planned to be built at Dongguan, Guangdong province in southern China. Due to limited initial funding, prototype R&D on key accelerator components is staged in two periods. With the initial funds of about 30 million CNY (about US$4M), we started period-I design, prototyping and testing of some major components of the accelerator system (a section of the DTL tank, two RCS magnets, a set of RCS dipole power supply, a RCS RF cavity, and a set of RCS ceramic vacuum ducts), the target system (target body, moderator and cooling system, decouple and poison), and the instrument system (background chopper, neutron guide, neutron detector). Project construction is expected to start in 2008 for a period of about 5 years.

Among physical, technical, and managerial challenges facing the project, the primary challenges are to complete the project as a first quality, reliable user's facility with a fraction of the "world standard" cost, and to reserve upgrade potential for future developments. To meet these challenges, we must keep the final component fabrication domestic as much as possible taking advantage of the relatively low labor cost, and seek worldwide collaborations for advanced technology.

ACCELERATOR SYSTEMS

The design of the accelerator complex is based on the experience at accelerator facilities including ISIS, PSR, SNS, J-PARC, the BNL AGS/Booster (Fig. 1), and the Beijing Electron Positron Collider (BEPC), and project proposals including the AUSTRON [15] and the ESS [16].

The initial H^- ion source needs to provide 0.5 ms long, 25 mA peak current, $0.2\pi\mu$m emittance ($\epsilon_{N,rms}$) pulses at 25 Hz to 50 keV energy for phase I. Two types of ion sources are considered best candidates for their favorable cost and reliability performance: the ISIS-type Penning surface source [17], and the DESY/modified-SNS-type RF driven source with external antenna [18, 19]. Owing to the kind support from the ISIS, we started to build the ISIS-type H^- Penning source body to be initially tested at ISIS. A pre-chopper in the LEBT is designed to chop the beam macropulse at a 50% ratio at the ring injection revolution period.

Originally, the RF frequency of the linac was 352 MHz based on available cw klystron and waveguide equipment assisted by CERN. However, the pulsed feature of the beam demands a linac RF source of higher peak power for efficiency. The RF frequency for the linac is thus changed to 324 MHz, the same as that of J-PARC so that the same klystron can be used for the RFQ and DTL. This frequency also gives a reasonable room for the EM quadrupole inside the drift tube.

The four-vane RFQ is similar to the one previously developed at IHEP for the Accelerator Driven Sub-critical (ADS) program [20] (Fig. 3). In comparison, the input energy is lowered to 50 keV to ease chopping. Space is reserved in the Medium Energy Beam Transport (MEBT) to house both the secondary chopper and beam halo scraper for phase II and beyond when the beam intensity is higher.

The DTL accelerates the 3 MeV beam from the RFQ to 81 MeV ([21]). Each of the four tanks consumes about the same amount of RF power (cavity RF power of 1.5 MW, total RF power of 2.0 MW). To reach a high effective shunt impedance, we vary the cell shape with β stepwise while keeping the maximum surface field below 1.3 times the Kilpatrick limit. J-PARC type EM quadrupoles made of electroformed hollow coils are used [22].

Five sets of power sources are used to power the RFQ and four DTL tanks. At 324 MHz RF frequency and 2.5 MW peak power, the Toshiba E3740A klystron is one of the candidates [23]. An ac series resonance high-voltage

Figure 3: The 3.5 MeV, ADS RFQ under commissioning at IHEP, China. The first proton beam was injected from the ECR ion source and successfully extracted with a transmission efficiency of about 92% on a proton beam of 43 mA peak current. The beam duty factor reached 6% with beam of 1.2 ms pulse length running at 50 Hz.

power supply is under development for the klystrons avoiding step-up high voltage transformers and multiphase high voltage rectifiers [24].

The Linac to Ring Beam Transport (LRBT) serves several functions [25]. The debuncher located at a distance from the end of linac reduces energy deviation and fluctuation. The 45° bend facilitates momentum collimation of possible beam halo and tail in the longitudinal direction. Three sets of scrapers provide collimation in the transverse directions. Finally, the beam is matched to phase-space parameters for ring injection downstream of the 45° anti-bend. The 45° bends sufficiently isolate the ring from the linac so that construction or maintenance may be performed on the ring while the beam is present in the linac. The bend also provides outlets of the linac beam for future applications.

Fig. 4 shows the layout of the RCS ring. A four-fold symmetric lattice is favored over three-fold to separate injection, collimation, and extraction to different straights. The ring adopts a hybrid lattice with missing-dipole FODO arcs and doublet straights (Fig. 5 [27, 28]). The dispersion is suppressed by using two groups of 3 half-cells (with 90° horizontal phase advance per cell) located on each side of a missing-dipole half-cell [28]. The long (one 9 m and two 6 m uninterrupted drifts per straight) dispersion-free straights facilitate injection [29], extraction [29], and transverse collimation. The FODO arcs allow easy lattice optics correction. The 4 m gap created by the missing dipole near the maximum dispersion location allow efficient longitudinal collimation [28].

The transverse acceptance is $350\pi\mu$m at the collimator and ring extraction channel, and $540\pi\mu$m elsewhere in the ring. The expected space-charge tune spread is about 0.2 for a beam of $320\pi\mu$m emittance. The momentum acceptance in $\Delta p/p$ is $\pm 1\%$ at the longitudinal collimator, and

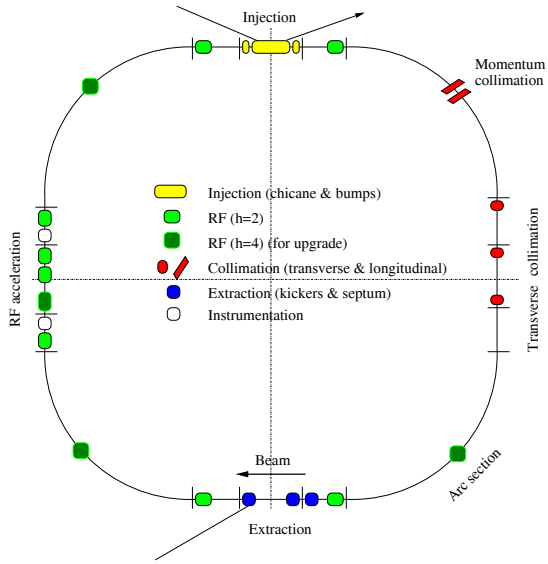

Figure 4: Functional layout of the CSNS RCS ring.

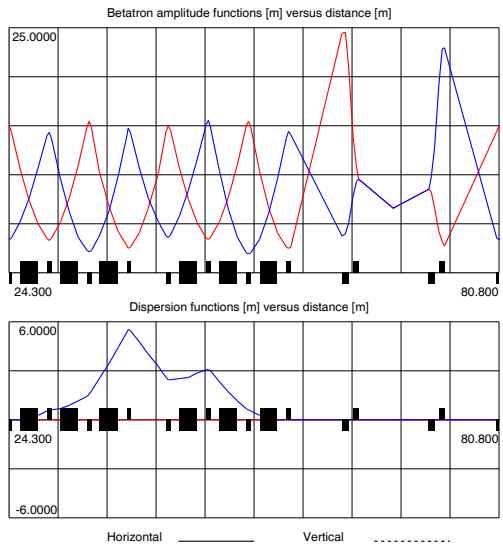

Figure 5: CSNS synchrotron lattice functions in one superperiod. The ring has a periodicity of 4.

$\pm 1.5\%$ elsewhere for a beam of $320\pi\mu$m emittance [30].

The acceleration is performed by 8 RF cavities with maximum total voltage of 165 kV per turn at harmonic $h = 2$. The main dipole field varies from 0.16 to 0.98 T. The bunching factor varies from 0.38 at injection to 0.12 at extraction. Chopping at 50% rate significantly reduces the expected beam loss occurring mostly during initial ramping. Space is reserved to house the second harmonic ($h = 4$) RF cavities to increase the bunching factor allowing a higher total beam intensity (Fig. 4).

The ring contains 24 main dipoles, 48 quadrupoles, 16 sextupoles, 32 trim quadrupoles, 32 multi-coil correctors, and injection and extraction magnets. With a high field (maximum dipole field of 0.98 T) and large aperture (dipole gap height of 178 mm and quadrupole pole radius from 209

to 308 mm) main magnet prototyping is in progress starting with J-PARC type stranded aluminum wires fabricated by domestic vendors. So far, three domestic vendors have successfully fabricated RCS dipole magnet coils made of such wires (Fig. 6). This type of coil will be used for the prototype ring dipole magnet. For the ring quadrupole magnet, we pursue in parallel designs with stranded aluminum wires and with four-piece hollow-conductor copper wires. A comparison will be made to determine the most robust and cost effective quadrupole magnet design.

Figure 6: One of the first prototypes of the J-PARC type stranded magnet coil fabricated by a vendor in China.

The ring main magnets are powered by a family of dipole and 8 families of quadrupole power supplies arranged in parallel groups with multimesh White circuits operating at 25 Hz resonance [31]. The demand for stability and matching is high (THD $<0.02\%$, stability $<0.1\%$). The trim quadrupoles and correctors are expected to play important roles in orbit and tune controls during the ramp cycle [26]. The sextupoles are dc powered for chromatic correction mainly at injection.

The ring RF system uses ferrite-loaded cavities to meet phase I ($h = 2$) requirements [32]. The design gradient is about 10 kV/m. Test stands are set up to measure the ferrite properties under the dynamic ramp cycle.

Ceramic ducts are chosen for the ring vacuum chambers under magnets to alleviate heating and field distortion caused by the eddy current, and to resist the impact of possible high-power beam loss. Both ISIS-type glass joint and J-PARC type metallic brazing are under study to form long, curved, large-bore ducts. Detachable, external metal-stripe wrappings are considered for the RF shielding, and all inner surfaces (ceramic, metal, and ferrite) are to be coated with TiN to reduce secondary electron emission yield [2].

The injection adopts SNS-type scheme with phase-space painting using 4 shift dipoles and 8 painting bump magnets [29, 33]. For simplicity, we consider using dc shift dipoles instead of 25 Hz ac. The beam-dynamics impact of the closed bump with its amplitude reducing with energy ramping is expected to be small. Excessive foil hits are avoided by displacing the orbit from the corner-located foil immediately upon the injection completion using the painting bumps powered by IGBT-based programmable supplies.

The extraction adopts SNS-type single-turn extraction with vertical kicking and horizontal bending. The kicker system consists of lumped, in-vacuum ferrite modules powered by dual PFN charging supplies. The Lambertson-type septum avoids possible damage caused by beam loss on the magnet coil.

For beam diagnostics we plan a suite of instruments similar to those of SNS, starting with allocating space and specifying accelerator-physics requirements. For accelerator controls, machine protection, and commissioning applications we build from the experience of BEPC/BEPCII and SNS projects (adopting EPICS, XAL, PSI/PSC control, static and dynamic databases, etc.).

TARGET SYSTEMS

With a design beam power of about 200 kW, CSNS uses a heavy water-cooled tungsten plat target surrounded by a beryllium-iron reflector, three wing-moderators (decoupled water at the room temperature, coupled hydrogen at 20 K and decoupled-poisoned methane at 100 K), bulk shields and neutron-scattering facilities, as shown in Fig. 7 [35]. Proton pulses from the accelerator impinge on the target, and the resulting spallation process produces large quantities of fast neutrons. The moderators slow these neutrons down to energies suitable for neutron scattering. 18 ports with vertical steel shutters are designed in the iron-heavy-concrete shielding passing neutrons for the instruments. A trolley system is designed to move the target vessel out of the main shielding for maintenance.

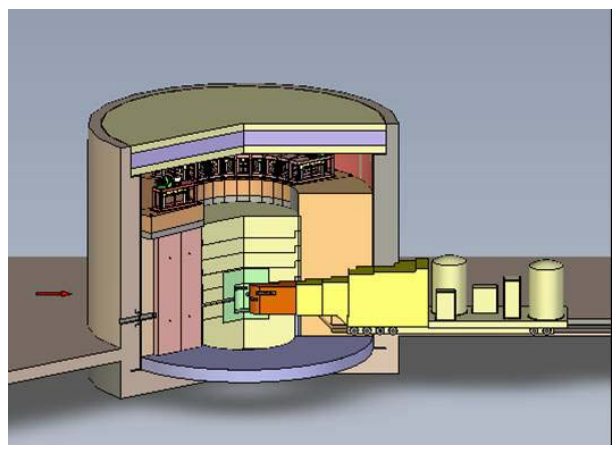

Figure 7: CSNS target station layout.

Tungsten is a proven target material for a facility with beam power of 100 to 200 kW. However, cladding with tantalum is necessary due to material brittleness caused by radiation damage and corrosion by heavy water coolant. Cladding using hot isostatic press and plasma spraying methods are attempted. Meanwhile, we study tungsten-rhenium alloy as alternative target material. Such alloy still has high charge state and mass density to provide a high neutron flux, and yet is expected to be resistant to radiation and thermal damage [36].

INSTRUMENT SYSTEMS

As shown in Fig. 8, so far 17 neutron scattering instruments are selected according to user demands and mod-

erator specifications: 6 powder neutron diffractometers, a single crystal diffractometer, a small angle neutron scattering diffractometer, two reflectometers, three direct geometry inelastic neutron scattering spectrometers, and four reversal geometry inelastic neutron scattering spectrometers [37]. The remaining beam line from liquid hydrogen moderator is reserved for basic neutron physics and/or neutron radiography. Among these 18 instruments, five day-one instruments are supported by the limited project funds: a high intensity diffractometer, a high resolution diffractometer, a broad Q-range small angle diffractometer, a multi-purpose reflectometer, and a direct geometric inelastic spectrometer.

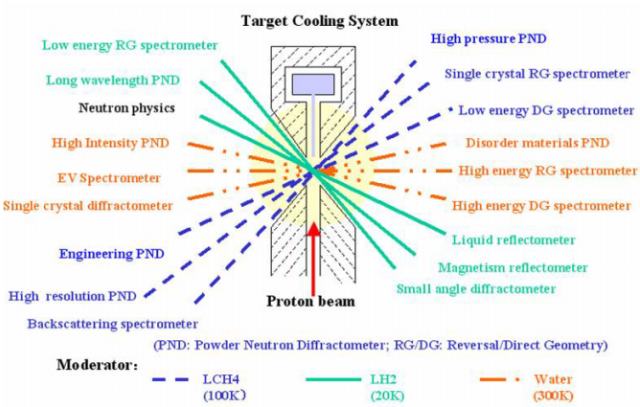

Figure 8: CSNS instrument layout.

FUTURE OUTLOOK

The CSNS is designed to provide beam power up to 500 kW in phased stages capable of supporting one or more target stations. Power upgrade depends crucially on maintaining low uncontrolled beam loss. The upgrade beyond phase I will mainly be realized by raising the linac energy to allow a higher beam intensity under the same ring space-charge limit, and by adding the second harmonic RF to increase the bunching factor in the ring.

It is possible for CSNS to serve multiple purposes including serving as a test facility for the ADS (ADTF). Fig. 9 shows a possible layout with ADTF receiving test beams from the CSNS linac, CSNS ring, and a dedicated high-duty linac. Extension of the linac provides higher power, while extension of the ring yields higher energies.

We thank colleagues and friends around the world for their generous help on the CSNS project.

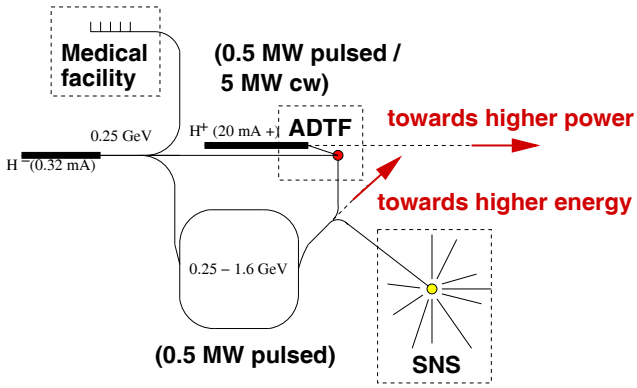

Figure 9: Possible CSNS upgrades towards higher power, higher energy, and multipurpose.

REFERENCES

[1] *Handbook of Accelerator Physics and Engineering*, ed. A. Chao and M. Tigner (World Scientific, Singapore, 2006)
[2] J. Wei, Rev. Mod. Phys. **75** (2003) 1383; J. Wei et al, PRST-AB, **3** (1999) 080101
[3] G.S. Bauer et al, PAC (1997) 3785
[4] ICANS XII (1993), RAL Proc. 94-025; ICANS XIII (1995), PSI Proc. 95-02
[5] B.-H. Choi, APAC (2004) 231
[6] G.H. Rees, PAC (1993) 731
[7] P. Bryant, PAC (1995) 322
[8] N. Holtkamp, EPAC (2006) 29
[9] I.S.K. Gardner, EPAC (1994) 3
[10] JAERI-Tech 2003-044, KEK Report 2002-13 (2003)
[11] I.S.K. Gardner et al, PAC 97 (1997) 988
[12] IHEP Report IHEP-CSNS-Report/2004-01E (2004)
[13] S.-X. Fang et al, J. Korean Phys. Soc. **48**(4) (2006) S697
[14] J. Zhang, Q.W. Yan, C. Zhuang et al, J. Neutron Research 13, 11 (2005)
[15] P.J. Bryant, et al. eds., *AUSTRON Feasibility Study* (1994)
[16] *The European Spallation Source Project Technical Report* (ESS Council, 2002)
[17] R. Sidlow et al, EPAC (1996) THP084L; G.E. Derevyankin, V.G. Dudnikov, AIP Conf. Proc. No. 111 (New York, 1984) 376; D.C. Faircloth et al, PAC (2005) 1910
[18] J. Peters, LINAC (1996) 199
[19] R. Keller et al, PAC (2001) 70; R.F. Welton et al, PAC (2005) 472
[20] S.-N. Fu et al, J. Korean Phys. Soc. **48**(4) (2006) S806
[21] S. Fu et al, LINAC (2006, to be published)
[22] H. Ino et al, LINAC (2000) 1015; K. Yoshino et al, LINAC (2000) 569; F. Naito et al, LINAC (2002) 361
[23] Toshiba Elec. Tubes Dev. Co. Ltd., www.toshiba-tetd.co.jp
[24] J. Li, Z. Zhang, et al, CSNS Tech. note (2006)
[25] J.-Y. Tang et al, EPAC (2006) 1780
[26] C.M. Warsop, AIP Conf. Proc. 448 (New York, 1998) 104
[27] S. Wang et al, EPAC (2006) 1996
[28] J. Wei et al, EPAC (2006) 2074
[29] J.-Y. Tang et al, EPAC (2006) 1783; 1777
[30] N. Wang, Q. Qin, these proceedings
[31] X. Qi, Ph. D. dissertation, IHEP, CAS (2006)
[32] H. Sun, W.L. Huang, et al, Tech. note BSNS/ACC-RR-343-01 (2006)
[33] J. Qiu et al, EPAC (2006) 1774
[34] L. Young, PAC (1993) 3136
[35] Q.W. Yan, W. Yin, B.L. Yu, ICANS (2003) 25
[36] X.J. Jia, Q.W. Yan, 8th Intern. Workshop on Spallation Materials and Technology (2006, Taos, NM, USA)
[37] F.W. Wang, P.L. Zhang, Q.W. Yan, ICANS (2003) 345; F. W. Wang, et al., ICANS (2005) 968